Monthly Notices
of the
ROYAL ASTRONOMICAL SOCIETY

MNRAS **430,** 1247–1256 (2013) doi:10.1093/mnras/sts705

Probing the blow-off criteria of hydrogen-rich 'super-Earths'

H. Lammer,[1]⋆ N. V. Erkaev,[2,3] P. Odert,[1,4] K. G. Kislyakova,[1,4] M. Leitzinger[4] and M. L. Khodachenko[1]

[1]*Space Research Institute, Austrian Academy of Sciences, Schmiedlstr. 6, A-8042 Graz, Austria*
[2]*Institute for Computational Modelling, Russian Academy of Sciences, Krasnoyarsk 36, Russia*
[3]*Siberian Federal University, Krasnoyarsk 36, Russia*
[4]*Institute of Physics, University of Graz, Universitätsplatz 5, A-8010 Graz, Austria*

Accepted 2012 December 20. Received 2012 November 19; in original form 2012 October 1

ABSTRACT

The discovery of transiting 'super-Earths' with inflated radii and known masses, such as Kepler-11b-f, GJ 1214b and 55 Cnc e, indicates that these exoplanets did not lose their nebula-captured hydrogen-rich, degassed or impact-delivered protoatmospheres by atmospheric escape processes. Because hydrodynamic blow-off of atmospheric hydrogen atoms is the most efficient atmospheric escape process we apply a time-dependent numerical algorithm which is able to solve the system of 1D fluid equations for mass, momentum and energy conservation to investigate the criteria under which 'super-Earths' with hydrogen-dominated upper atmospheres can experience hydrodynamic expansion by heating of the stellar soft X-rays and extreme ultraviolet (XUV) radiation and thermal escape via blow-off. Depending on orbit location, XUV flux, heating efficiency and the planet's mean density our results indicate that the upper atmospheres of all 'super-Earths' can expand to large distances, so that except for Kepler-11c all of them experience atmospheric mass-loss due to Roche lobe overflow. The atmospheric mass loss of the studied 'super-Earths' is one to two orders of magnitude lower compared to that of 'hot Jupiters' such as HD 209458b, so that one can expect that these exoplanets cannot lose their hydrogen envelopes during their remaining lifetimes.

Key words: hydrodynamics – planets and satellites: atmospheres – planets and satellites: physical evolution – planet-star interactions – ultraviolet: planetary systems – ultraviolet: stars.

1 INTRODUCTION

The detection of hydrogen- and volatile-rich exoplanets at orbital distances <1 au opens questions regarding their upper atmosphere structures and the stability against escape of atmospheric gases. Since $\geq$40 per cent of all discovered exoplanets are orbiting their host stars at distances closer than the orbit of Mercury, the atmospheres of these bodies evolve in much more extreme environments than what is known from the planets in our Solar system. More intense stellar X-ray, soft X-ray, extreme ultraviolet (EUV)[1] radiation and particle fluxes at such close orbital distances will alter the upper atmosphere structure of these objects to a great extent.

Lammer et al. (2003) were the first to provide a model of exoplanetary upper atmospheres, which is based on an approximate solution of the heat balance equation in planetary thermospheres (Bauer 1971; Gross 1972) and found that hydrogen-rich upper atmospheres of Jupiter-type gas giants in close orbital distances will be heated to several thousands of kelvin, so that hydrostatic conditions cannot be valid anymore, because the planet's upper atmosphere will expand dynamically upwards. Under such conditions the exobase can move to locations which are above a possible magnetopause or even at the Roche lobe distance (e.g. Lammer et al. 2003; Lecavelier des Etangs et al. 2004; Erkaev et al. 2007; Lammer et al. 2009a), so that the upward-flowing neutral gas can interact with the dense stellar plasma flow (Holmström et al. 2008; Ekenbäck et al. 2010; Lammer et al. 2011). Hydrodynamic models by Yelle (2004), Tian et al. (2005a), García Muñoz (2007), Penz et al. (2008a) and Koskinen et al. (2010) agreed also with the hypothesis of Lammer et al. (2003, 2009a) that close-in hydrogen-rich exoplanets experience dynamic atmospheric expansion and outflow up to their Roche lobes with mass-loss rates in the order of $\sim$(1–5) $\times$ 10^{10} g s^{-1}.

The first observational evidence of an XUV-heated extended non-hydrostatic upper atmosphere was obtained for the hot gas giant HD 209458b, which orbits a Sun-like star at 0.047 au (Vidal-Madjar et al. 2003; Ben-Jaffel 2007; Ben-Jaffel & Sona Hosseini 2010). Excess absorption in the Lyman α line of $\sim$9–15 per cent during the transit was interpreted as being caused by a population of atomic hydrogen located beyond the Roche lobe, indicating a hot and extended upper atmosphere. Subsequent detection of O I and C II by

⋆ E-mail: helmut.lammer@oeaw.ac.at

[1] The radiation between 5 and 920 Å contains soft X-rays and EUV and is considered as XUV radiation.

Vidal-Madjar et al. (2004), as well as Si III by Linsky et al. (2010) supports the hypothesis that these heavy elements are likely to be carried there from deeper atmospheric levels with the dynamical hydrogen flow. Metals have been found around the Roche lobe of the highly irradiated 'hot Jupiter' WASP-12b, an inflated gas giant at ∼0.023 au, by Fossati et al. (2010). As heavier elements can only be dragged to the upper atmosphere regions along with upwards flowing hydrogen atoms, these observations of heavy elements at large distances from the planet most likely confirm scenarios which were suggested by Sekiya, Nakazawa & Hayashi (1980), Sekiya, Hayashi & Nakazawa (1981), Hunten, Pepin & Walker (1987) and Pepin (1991, 2000) that hydrodynamic escape from early Solar system planets like Venus could have generated Ne and Ar isotope ratios close to the observed values in its present-time atmosphere and noble gas ratios similar to those derived for Earth's initial atmosphere. In view of atmospheric isotope studies it is generally accepted that hydrodynamic outflow driven by the XUV-active young Sun could have been responsible for the observed heavy isotope enrichment in the atmospheres of Venus, Earth and Mars (e.g. Lammer et al. 2008, and references therein).

Therefore, depending on the activity of a planet's host star, its orbit location, mass and size, one can expect that some exoplanets experience high atmospheric mass loss during their lifetimes (Lammer et al. 2003; Vidal-Madjar et al. 2003, 2004; Baraffe et al. 2004; Lecavelier des Etangs et al. 2004, 2010; Yelle 2004; Tian et al. 2005a; Erkaev et al. 2007; García Muñoz 2007; Hubbard et al. 2007; Khodachenko et al. 2007; Koskinen, Aylward & Miller 2007; Lecavelier des Etangs 2007; Penz et al. 2008; Penz, Micela & Lammer 2008b; Penz & Micela 2008; Davis & Wheatley 2009; Lammer et al. 2009a; Murray-Clay, Chiang & Murray 2009; Fossati et al. 2010; Linsky et al. 2010; Leitzinger et al. 2011; Owen & Jackson 2012).

In this context, the discoveries of very close-in low-mass exoplanets like CoRoT-7b (e.g. Léger et al. 2009) and Kepler-10b (e.g. Batalha et al. 2011) at <0.02 au raise the question whether these objects have always been so-called 'super-Earths', or if are they just remnants of once more massive gaseous planets which lost their whole hydrogen envelopes (e.g. Jackson et al. 2010; Valencia et al. 2010; Leitzinger et al. 2011). However, besides rocky 'super-Earths' which orbit at very close orbital distances such as CoRoT-7b, Kepler-10b, Kepler-18b (Cochran et al. 2011) and planets in the Kepler-20 system (Fressin et al. 2012), the Kepler space observatory discovered several low-density 'super-Earths' closely packed in the Kepler-11 system (Lissauer et al. 2011), whose mean densities indicate that they have rocky cores which are surrounded by significant amounts of hydrogen/helium envelopes (e.g. Lissauer et al. 2011; Lammer 2012; Lammer et al. 2012; Ikoma & Hori 2012). Moreover, the mean densities of other transiting 'super-Earths', such as GJ 1214b (Charbonneau et al. 2009) or 55 Cnc e (Demory et al. 2012; Endl et al. 2012; Gillon et al. 2012), also indicate substantial envelopes of light gases such as hydrogen and He or H_2O. For GJ 1214b, the current status of observational evidence supports mainly two possible atmospheres, namely an H/He-dominated atmosphere with clouds and low methane content, or an H_2O-dominated atmosphere (Bean, Miller-Ricci & Homeier 2010; Bean et al. 2011; Croll et al. 2011; Désert et al. 2011; de Mooij et al. 2012). For the large 'super-Earth' 55 Cnc e three different composition-based hypotheses can be found in the literature, within the first two possibilities are a rocky planet with an H/He dominated atmosphere, or a supercritical water planet (Demory et al. 2012; Gillon et al. 2012). The third hypothesis is based on a recent study by Madhusudhan, Lee & Mousis (2012) where these authors suggest that the mass and radius of 55 Cnc e can also be explained by a carbon-rich solid interior made of Fe, C, SiC and/or silicates and without a volatile envelope. Although there may be this possibility of an alternative more exotic explanation for 55 Cnc e, the discoveries of these low-density hydrogen and/or H_2O-rich planets can be seen as an indication that many 'super-Earths' even located close to their host stars will not lose their initial volatile-rich protoatmospheres during their lifetimes (Ikoma & Hori 2012; Lammer 2012). If so, the consequences of these findings are very relevant for the probability and evolution of Earth-type class I habitats (Lammer et al. 2009b; Lammer 2012) and habitability in general (Pierrehumbert & Gaidos 2011; Wordsworth 2012). Understanding the efficiency of atmospheric loss processes at hydrogen-rich 'super-Earths' is therefore crucial.

The aim of this study is to investigate the environmental conditions under which 'super-Earths' with hydrogen-rich upper atmospheres undergo hydrodynamic blow-off. For this study we focus only on 'super-Earths' for which the sizes and masses are more or less well determined. For that reason we do not include transiting 'super-Earths' such as HD 97658b, Kepler-9d, or small terrestrial planets such as those discovered in the Kepler-42 system with unknown or uncertain masses, or 'super-Earths' with known masses but unknown radii.

In Section 2 we describe the adopted stellar and planetary input parameters and the hydrodynamic upper atmosphere model which is applied for the investigation of Kepler-11b, Kepler-11c, Kepler-11d, Kepler-11e, Kepler-11f, GJ 1214b and experience atmospheric blow-off or less efficient Jeans escape. In the controversial case regarding the composition of 55 Cnc e, we assume in this study that the planet is surrounded by a hydrogen envelope, which would be the case if rocky core of the planet is surrounded by an H/He, or H_2O dominated atmosphere as suggested by Demory et al. (2012) or Gillon et al. (2012).

In Section 3 we apply our hydrodynamic model to these low-density 'super-Earths' and study the response of their upper atmospheres to the stellar XUV flux and calculate the thermal atmospheric escape rates. We compare our results to the widely used energy-limited blow-off formula and discuss the relevance of our findings for 'super-Earths' in general.

2 INPUT PARAMETER AND MODEL DESCRIPTION

2.1 XUV fluxes of Kepler-11, GJ 1214 and 55 Cnc

Unfortunately, the XUV fluxes of the host stars of the studied 'super-Earths' are not very well constrained. The XUV emission of Kepler-11, a slightly evolved late-G star (Lissauer et al. 2011), is observationally unconstrained, because its large distance (>600 pc) and high age (6–10 Gyr) prevent detection by current instruments. Hence, we estimate its XUV flux via its age by using power laws from Ribas et al. (2005), although we caution that application of these calibrations for stellar ages higher than about 6.7 Gyr (the highest age in their sample) might introduce additional uncertainties because of the extrapolation to an even older, slightly evolved G star. Adopting a mean age of 8 Gyr, this approach yields a log $L_{\rm XUV} \approx 27.81\,{\rm erg\,s^{-1}}$, which corresponds to fluxes of $F_{\rm XUV} \sim 278$, 204, 91, 61, 37 erg cm^{-2} s^{-1} at the respective orbits of the Kepler-11 planets b-f. We estimate the uncertainties of these values to be at least an order of magnitude due to the extrapolation of the calibrations and the just loosely constrained stellar age.

Table 1. Planetary and stellar model input parameters for Kepler-11b-f (Lissauer et al. 2011; http://kepler.nasa.gov/Mission/discoveries/), GJ 1214b (Charbonneau et al. 2009) and 55 Cnc e (Demory et al. 2012; Endl et al. 2012; Gillon et al. 2012). $I_{\rm XUV}$ corresponds to the stellar XUV flux at the planetary orbits normalized to the solar value at 1 au.

Exoplanet	d (au)	$I_{\rm XUV}$	$R_{\rm pl}$ ($R_\oplus$)	$M_{\rm pl}$ ($M_\oplus$)	$\rho_{\rm pl}$ (g cm^{-3})	T_0 (K)
Kepler-11b	0.091	60	1.97	4.3	3.1	∼900
Kepler-11c	0.1	45	3.15	13.5	2.3	∼833
Kepler-11d	0.159	20	3.43	6.1	0.9	∼692
Kepler-11e	0.195	13	4.52	8.4	0.5	∼617
Kepler-11f	0.25	8	2.61	2.3	0.7	∼544
GJ 1214b	0.014	470	2.67	6.55	1.87	∼475
55 Cnc e	0.0156	1060	2.17	8.37	4.56	∼2360

Although GJ 1214 is located at a closer distance (∼13 pc), the star has not been detected in X-rays up to now. This is probably due to the intrinsic faintness of this M4.5V star and its age of 3–10 Gyr (Charbonneau et al. 2009). Therefore, we use the relation between X-ray luminosity and age of Engle & Guinan (2011) calibrated for M dwarfs. This relation yields an X-ray luminosity of $\log L_{\rm X} \approx 26.8\,{\rm erg\,s^{-1}}$ for an adopted age of 6 Gyr. To correct for the unknown EUV emission, we assume that the contributions to the total XUV flux of both X-rays and EUV are ∼50 per cent each, typical for moderately active stars (e.g. Sanz-Forcada et al. 2011), but EUV can make up to 90 per cent of the emission for inactive stars. This leads to an estimated XUV flux at GJ 1214b's orbit of $F_{\rm XUV} \approx 2200\,{\rm erg\,cm^{-2}\,s^{-1}}$. As for Kepler-11, the uncertainty of this value also corresponds at least an order of magnitude because of the large range of possible stellar ages, the intrinsic spread of about one order of magnitude of coeval stars of the same mass, and the very crude correction applied for the unknown EUV emission.

For 55 Cnc, a nearby (∼12.5 pc) G9IV star (von Braun et al. 2011), X-ray emission was detected by ESA's *XMM–Newton* space observatory (Sanz-Forcada et al. 2011). These authors used X-ray spectra of numerous planetary host stars to extrapolate their EUV emission by using calibrations of stars with well-determined emission measure distributions (EMD). They estimated a total XUV luminosity within the wavelength region 5–920 Å of $\log L_{\rm XUV} = 27.55^{+0.46}_{-0.42}\,{\rm erg\,s^{-1}}$, which translates to an XUV flux of $F_{\rm XUV} \approx 4913\,{\rm erg\,cm^{-2}\,s^{-1}}$ at the orbit of 55 Cnc e. The uncertainty is ≥50 per cent, mainly due to the uncertainties in the extrapolated transition region EMD. Although X-rays might contribute somewhat to the heating of the lower thermosphere, from our analysis of the available data we assume that for the particular atmospheric escape of the investigated planets is mainly driven by the stellar EUV emission. This assumption is supported by the fact that for rather old stars like the ones studied here, however, the major portion of the XUV flux (80–90 per cent) is emitted in the EUV range.

The properties of the studied planets are summarized in Table 1, which also gives the XUV enhancement factors $I_{\rm XUV}$, corresponding to the ratio of the adopted XUV fluxes at the planet's orbits normalized to the present XUV flux of the Sun at 1 au ($4.64\,{\rm erg\,cm^{-2}\,s^{-1}}$; Ribas et al. 2005).

2.2 Energy absorption and model description

The energy budget of upper planetary atmospheres is mainly governed by the heating of the bulk atmosphere due to the absorption of the XUV radiation (e.g. Bauer & Lammer 2004) and in very close orbital distances also harder X-rays (Cecchi-Pestellini et al. 2009; Owen & Jackson 2012) by atmospheric constituents, by heat transport due to conduction and convection and by heat loss due to emissions in the infrared (IR). Because the XUV fluxes are based on only rough estimates except for 55 Cnc e, and the atmospheric composition of the studied planets is not very well constraint, we do not consider a wavelength dependent derivation of the heating function. But we note that for future studies of exoplanets with known XUV spectra and atmospheric composition it might be important to investigate the influence of wavelength dependent absorption cross-sections and their impact on the upper atmosphere structure. The volume heat production rate $q_{\rm XUV}$ due to the absorption of the stellar radiation for given wavelengths and constituents can then be written as

$$q_{\rm XUV} = \eta n \sigma_{\rm a} J_{\rm XUV} {\rm e}^{-\tau}, \quad (1)$$

where $J_{\rm XUV}$ is the energy flux related to the corresponding wavelength range outside the atmosphere, $\sigma_{\rm a}$ is the appropriate hydrogen absorption cross-section which lies typically within the range of $\sim 10^{-18}$ to $6 \times 10^{-18}\,{\rm cm^2}$, and τ is the optical depth in the upper atmosphere and n the number density. η is the so-called heating efficiency or fraction of absorbed stellar radiation which is transformed into thermal energy and lies within in the range of ∼15–60 per cent (Chassefière 1996a,b; Yelle 2004; Lammer et al. 2009a; Leitzinger et al. 2011; Koskinen et al. 2012).

The value of η is also related to the availability of IR-cooling molecules such as CO_2, H_3^+, etc. and will then be closer to the lower value because less energy can be transferred into heat due to cooling by IR-emitting molecules. In a recent study by Koskinen et al. (2012), who applied a thermosphere model that calculates the heating rate based on the absorption of stellar XUV radiation and photoelectron heating efficiencies and photochemistry to the hydrogen-rich gas giant HD 209458b, it was found that η is most likely in the order of ∼40–60 per cent. For hydrogen-rich exoplanets which are exposed to XUV fluxes ≥100 times higher compared to that of the present Sun most molecules in the thermosphere are dissociated so that IR-cooling becomes less important yielding η ∼40–60 per cent. As this is the case for HD 208459b, IR-cooling by H_3^+ molecules can be neglected (Koskinen et al. 2007). However, for the Kepler-11 'super-Earths' which are exposed to XUV fluxes ∼8–60 times higher than today's Sun, depending on the availability of potential IR-cooling molecules, η may be closer to the lower value of 15 per cent.

As mentioned in Section 2, it is also necessary to check if escape by X-ray heating could be relevant for the studied 'super-Earths'. However, as X-ray heating usually dominates at young stellar ages (Owen & Jackson 2012), it is unlikely to be of relevance here because of the rather high ages of the host stars. If we compare the X-ray luminosities of the host stars with the values necessary for having dominating X-ray escape (Owen & Jackson 2012; their fig. 11), one can estimate that X-ray luminosities of at least 10^{28} or $10^{30}\,{\rm erg\,s^{-1}}$ would be necessary for the close-in GJ 1214b and 55 Cnc e 'super-Earths' and the further separated Kepler-11b-f planets, respectively, if we adopt the values for a Neptune-mass planet with a density of $1\,{\rm g\,cm^{-3}}$ as a lower limit. The X-ray luminosities of all studied 'super-Earth' host stars are all well below these values ($<10^{27}\,{\rm erg\,s^{-1}}$). Therefore, we assume that X-ray induced evaporation can be neglected or may play a minor role for the studied 'super-Earths', and XUV radiation should be responsible for the main heating processes in their hydrogen-rich thermospheres.

By averaging the XUV volume heating rate over the planet's dayside one obtains

$$q_{\rm XUV}(r) = \frac{\eta n \sigma_{\rm a}}{2} \int_0^{\frac{\pi}{2}+\arccos(\frac{1}{r})} J_{\rm XUV}(r,\Theta)\sin(\Theta)\,{\rm d}\Theta, \quad (2)$$

with the polar angle Θ and $J_{\rm XUV}(r, \Theta) = J_{\rm XUV}{\rm e}^{-\tau}$. Because the thermal escape rate is determined by the total energy deposited in the upper atmosphere, which is given by the integral of the XUV volume heating rate over the radial distance within the simulation domain, the shape of $q_{\rm XUV}$ has a minor effect to the atmospheric loss rate. Besides the uncertainties in the availability of possible thermospheric IR-coolers, other parametrical uncertainties such as the chosen XUV flux, a possible X-ray heating contribution, the stellar age, etc. are most likely within the investigated limits of the assumed 15–40 per cent η range.

For studying the response of the hydrogen-dominated upper atmospheres of our 'super-Earths' to the stellar XUV flux we apply a non-stationary 1D hydrodynamic upper atmosphere model which is a further developed model based on Penz et al. (2008), and solves the system of the 1D fluid equations for mass, momentum and energy conservation in spherical coordinates.

$$\frac{\partial \rho r^2}{\partial t} + \frac{\partial \rho v r^2}{\partial r} = 0, \quad (3)$$

$$\frac{\partial \rho v r^2}{\partial t} + \frac{\partial \left[r^2(\rho v^2 + P)\right]}{\partial r} = \rho g r^2 + 2Pr, \quad (4)$$

$$\frac{\partial r^2 \left[\frac{\rho v^2}{2} + \frac{P}{(\gamma-1)}\right]}{\partial t} + \frac{\partial v r^2 \left[\frac{\rho v^2}{2} + \frac{\gamma P}{(\gamma-1)}\right]}{\partial r} = \rho v r^2 g + q_{\rm XUV} r^2, \quad (5)$$

with pressure

$$P = \frac{\rho}{m_{\rm H}} kT, \quad (6)$$

and gravitational acceleration,

$$g = -\nabla\Phi, \quad (7)$$

$$\Phi = -G\frac{M_{\rm pl}}{r} - G\frac{M_{\rm star}}{(d-r)} - G\frac{M_{\rm pl}+M_{\rm star}}{2d^3}\left(\frac{M_{\rm star}d}{M_{\rm star}+M_{\rm pl}} - r\right)^2. \quad (8)$$

Here, r corresponds to the radial distance from the planetary centre, and ρ, v, P and T are the mass density, radial velocity, pressure and temperature of the bulk atmosphere, respectively. $m_{\rm H}$ is the mass of the hydrogen atoms, k is the Boltzmann constant, G is Newton's gravitational constant, and γ is the polytropic index or the ratio of the specific heats.

For exoplanets at very close orbital distances one cannot neglect gravitational effects which are related to the Roche lobe (Erkaev et al. 2007; Penz et al. 2008; Lammer et al. 2009a). Although most of our studied 'super-Earths' have orbital locations closer than 0.1 au, due to their low gravity compared to Jovian-type planets, their upper atmospheres may expand to several planetary radii and probably reach the Roche lobe. Therefore, we include in our study also the Roche lobe related gravitational force, which we refer to as Roche lobe effects with planetary mass $M_{\rm pl}$ and mass of the host star $M_{\rm star}$ and orbital distance of the planet d. The upper atmospheres of planets can mainly be in two regimes. In the first, the thermosphere is in hydrostatic equilibrium where the bulk of the upper atmosphere gas below the exobase can be considered as hydrostatic. In the second, the upper atmosphere may hydrodynamically expand and the bulk atmospheric particles can escape efficiently as a result of high stellar XUV fluxes, and/or a weak planetary gravitational field (e.g. Lammer 2012). Under certain conditions and for certain planetary parameters the upper atmosphere can hydrodynamically expand, but the bulk velocity may not reach the escape velocity at the exobase level. In such cases one can expect a hydrodynamically expanding upper atmosphere but the loss rate results in a less efficient Jeans-type escape, but not in hydrodynamic blow-off (Tian et al. 2005b, 2008a,b). If the mean thermal energy of the upper atmosphere gases at the exobase level exceeds their gravitational energy, blow-off occurs (e.g. Öpik 1963).

Our simulation domain is limited by a lower boundary with a temperature T_0, density n_0 and a thermal velocity

$$v_0 = \left(\frac{kT_0}{m}\right)^{0.5} \quad (9)$$

at the homopause distance or base of the thermosphere. To estimate the temperature T_0 at the lower boundary one does not need to apply a full radiative transfer calculation because the temperature in this altitude region differs not greatly from the equilibrium or effective skin temperature

$$T_{\rm eq} = \left[\frac{S(1-A)}{\xi\sigma_{\rm B}}\right]^{0.25} \quad (10)$$

of the planet (e.g. Kasting & Pollack 1983; Bauer & Lammer 2004; Tian et al. 2005b). The factor ξ is 4 if a planet rotates fast and 2 for slowly rotating or tidally locked planets. Because the studied 'super-Earths' are within Mercury's orbit, it is likely that they rotate slower compared to the Earth so that ξ may be <4. $\sigma_{\rm B}$ is the Stefan–Boltzmann constant, A the albedo and S the stellar flux density which is the amount of the incoming electromagnetic radiation of the host star per unit area at the planet's orbit location. For the temperature T_0 at the lower boundary of the studied 'super-Earths' we use the estimated effective skin temperatures $T_{\rm eq}$ given in Table 1.

For planets close to or inside the habitable zone of a Sun-type G-star such as Venus or Earth this temperature is ∼230–250 K which is reached at an altitude of about 120 km.

Because of their low mean densities, in the case of GJ 1214b (Bean et al. 2010; Miller-Ricci & Fortney 2010; Nettelmann et al. 2010, 2011) and 55 Cnc e (Demory et al. 2012), it may be possible that these planets have a deep H_2O ocean which is possibly surrounded by a steam atmosphere. Such a scenario is not expected for the Kepler-11 low-density 'super-Earths'; these planets are most likely dominated by dense H/He envelopes (Lissauer et al. 2011; Ikoma & Hori 2012).

If a planet has a steam atmosphere the base of the thermosphere could also act as a kind of cold trap where the saturation H_2O mixing ratio reaches its minimum value. If a planet is dominated by a hydrogen-rich gas envelope or has different parameters compared to the Earth, the homopause altitude could also be somewhat higher, but the exobase location or escape rate at the top of the thermosphere should not greatly differ.

In the case of H_2/He dominated upper atmospheres there are three processes which can dissociate H_2 molecules into hydrogen atoms. The first process is thermal dissociation which becomes dominant when the atmospheric temperature reaches values >2000 K (Yelle 2004; Koskinen et al. 2010). The second process is photodissociation of hydrogen molecules which becomes dominant when the stellar EUV flux reaches values which are >25 times the present

solar value (Koskinen et al. 2010). The third possibility for the production of atomic hydrogen are photochemical reactions between CH_4 and other hydrocarbons taking place below the homopause level (e.g. Atreya 1986). A combination of photo-dissociation and photochemical reactions is responsible for the fact that H atoms are the dominant species in the upper atmosphere of Jupiter, Saturn, Uranus and Neptune. Because the studied 'super-Earths' are much hotter compared to the hydrogen-rich Solar system gas and ice giants are therefore exposed to higher photon fluxes and may also contain hydrocarbons in their lower atmospheres (Kuchner 2003) we assume that atomic hydrogen is the dominant species above their homopause levels.

In case the planet is surrounded by a dense hot steam atmosphere, the stellar XUV radiation dissociates the H_2O molecules above the mesopause via

$$H_2O + h\nu \rightarrow OH + H \quad (11)$$

and hydrogen atoms should also be the dominant species in the upper atmosphere (Kasting & Pollack 1983; Tian et al. 2005b; Lammer 2012). For the number densities n_0 we assume a hydrogen density of 10^{13} cm^{-3} similar as calculated for Saturn's, Uranus' and Neptune's homopause levels (Yamanaka 1995; Atreya 1999). This value is also comparable with the homopause hydrogen density of 5×10^{12} cm^{-3} which was adopted by Tian et al. (2005b) in a study of a hydrogen-rich early Earth, but slightly lower compared to that of Jupiter. This density value corresponds to an H_2O mixing ratio in Earth's atmosphere of 50 per cent which results, according to Kasting & Pollack (1983) and Tian et al. (2005b), also in an upper atmosphere which is dominated by hydrogen.

The upper boundary of our simulation domain is chosen at $45R_{\rm pl}$, but the results of our hydrodynamic model are considered as accurate only until the exobase level which is located where the mean-free path $l_{\rm c}$ reaches the scale height $H = (kT_{\rm exo})/(mg)$ of the hydrodynamically expanding upper atmosphere. Above the exobase level which separates the collision dominated thermosphere from the collision-less exosphere, hydrodynamics are not valid. If $\beta >$ 30 at the exobase level then an atmosphere is mainly bound to the planet and one can expect low thermal escape rates. Blow-off happens when β becomes <1.5 or the upper atmosphere reaches the Roche lobe distance (Öpik 1963; Chamberlain 1963; Bauer & Lammer 2004; Erkaev et al. 2007). For β values between ∼1.5 and 30, Jeans escape occurs but the upper atmosphere can expand within the hydrodynamic regime.

Because the classical Jeans formula is based on the isotropic Maxwellian distribution function, in case if the upper atmosphere expands dynamically but blow-off conditions are not established, we have the radial velocity of the outward flowing bulk atmosphere at the exobase, and thus a distribution function which is not isotropic. In such a case we calculate the Jeans-type escape rate by using a shifted Maxwellian function which is modified by the radial velocity v obtained from the hydrodynamic code (e.g. Volkov et al. 2011). We show the dynamically expanding upper atmosphere structures only up to the exobase levels.

3 RESULTS

The modelled XUV volume heating rates $q_{\rm XUV}$ for the seven 'super-Earths' with heating efficiencies $\eta = 15$ per cent and 40 per cent are shown in Fig. 1. Depending on the planets orbit location, equilibrium or skin temperature, and gravity, the peak of the XUV flux is deposited close to the planet or at higher altitudes. Corresponding to the volume heating rates the expected atmosphere

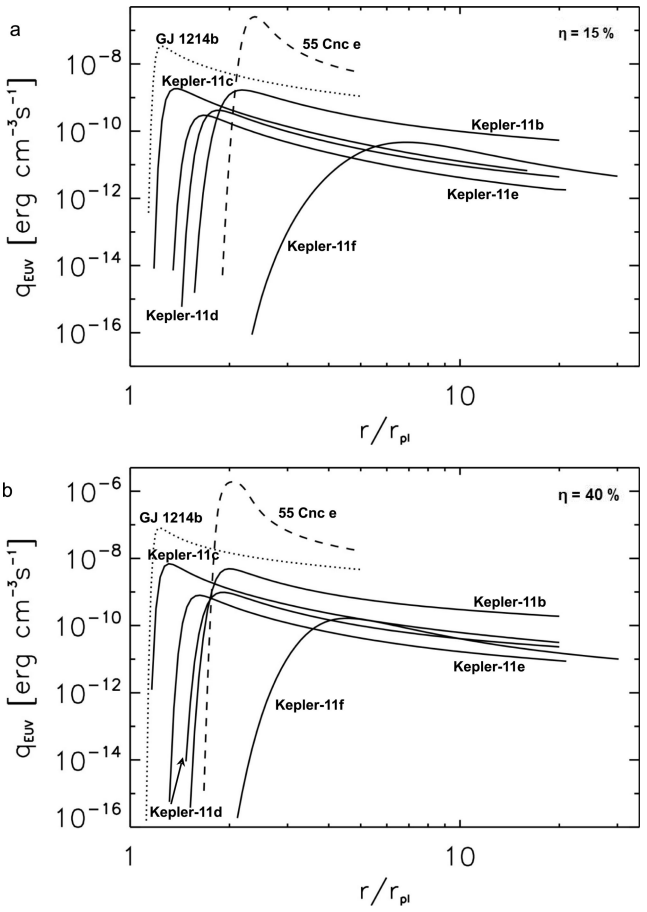

Figure 1. Calculated XUV volume heating rates $q_{\rm XUV}$ for 55 Cnc e (dashed line), GJ 1214b (dotted line), and the 5 Kepler-11 'super-Earths' (solid lines) as a function of distance in planetary radii for $\eta = 15$ per cent (a) and $\eta =$ 40 per cent (b), respectively.

temperature, velocity and density profiles as a function of planetary distance without (Table 2) and with the Roche lobe effects (Table 3) are then modelled. Table 2 shows the calculated exobase parameters $r_{\rm exo}$, $T_{\rm exo}$, $n_{\rm exo}$, the thermal escape rates $L_{\rm th}$ and mass-loss rates $\dot{M}_{\rm th}$ for the five 'super-Earths' in the Kepler-11 system, GJ 1214b and 55 Cnc e for heating efficiencies of 15 per cent and 40 per cent, respectively. For example, for Kepler-11f the exobase would be located at $\sim 117R_\oplus \sim 10R_{\rm Jup} \sim 1\,{\rm R}_\odot$. In the case of GJ 1214b which orbits around a M4.5 dwarf star with a radius of $\sim 0.21\,{\rm R}_\odot \sim 23R_\oplus$ the exobase would be located at $\sim 4.0R_{\rm GJ1214}$. This comparison indicates that the inflated upper atmosphere of GJ 1214b would cover the whole star during a transit. In the case of 55 Cnc e the expanding bulk atmosphere would reach escape velocity and hence blow-off conditions far below the estimated exobase level, so that the exobase location in that particular case is not relevant for the estimation of the thermal escape rate. For a heating efficiency η of 15 per cent blow-off would occur at $\sim 20R_{\rm pl}$ and for $\eta =$ 40 per cent at $\sim 14R_{\rm pl}$. Due to the lower gravity the combination of XUV heating and thermal expansion the exobase levels of Kepler-11b, Kepler-11d, Kepler-11e, Kepler-11f, GJ 1214b and 55 Cnc e move to distances which are far beyond the L_1 point $r_{\rm L1}$. Therefore, one cannot neglect Roche lobe effects for these particular 'super-Earths'. The thermal atmospheric escape rates for most planets are approximately two times higher if the heating efficiency η is

Table 2. Calculated exobase parameters without Roche lobe effects and thermal escape and mass-loss rates for the five 'super-Earths' of the Kepler-11 system, GJ 1214b and 55 Cnc e for heating efficiencies η of 15 per cent (upper part) and 40 per cent (lower part).

Parameter	Kepler-11b	Kepler-11c	Kepler-11d	Kepler-11e	Kepler-11f	GJ 1214b	55 Cnc e
Blow-off	Yes	No	Yes	Yes	Yes	Yes	Yes
r_{exo}/R_{pl}	∼33	∼14	∼27	∼25	∼41	∼35	∼ 136
T_{exo} (K)	∼1170	∼1000	∼415	∼430	∼50	∼4040	∼ 2230
n_{exo} (cm^{-3})	$\sim 6 \times 10^3$	$\sim 8 \times 10^3$	$\sim 5 \times 10^3$	$\sim 4 \times 10^3$	$\sim 1.6 \times 10^4$	$\sim 5 \times 10^3$	$\sim 1.75 \times 10^3$
L_{th} (s^{-1})	$\sim 5.6 \times 10^{31}$	$\sim 1.5 \times 10^{31}$	$\sim 6.0 \times 10^{31}$	$\sim 6.5 \times 10^{31}$	$\sim 2.0 \times 10^{32}$	$\sim 2.25 \times 10^{32}$	$\sim 9.5 \times 10^{32}$
$\dot{M}_{th}$ (g s^{-1})	$\sim 9.5 \times 10^7$	$\sim 2.43 \times 10^7$	$\sim 1.0 \times 10^8$	$\sim 1.1 \times 10^8$	$\sim 3.3 \times 10^8$	$\sim 3.45 \times 10^8$	$\sim 1.6 \times 10^9$
Blow-off	Yes	Yes	Yes	Yes	Yes	Yes	Yes
r_{exo}/R_{pl}	∼40	∼16	∼40	∼28	∼45	∼40	∼ 168
T_{exo} (K)	∼1800	∼1560	∼1040	∼680	∼55	∼7125	∼ 5530
n_{exo} (cm^{-3})	$\sim 6 \times 10^3$	$\sim 10^4$	$\sim 6 \times 10^3$	$\sim 5 \times 10^3$	$\sim 2 \times 10^4$	$\sim 6 \times 10^3$	$\sim 1.6 \times 10^3$
L_{th} (s^{-1})	$\sim 1.0 \times 10^{32}$	$\sim 4.5 \times 10^{31}$	$\sim 6.5 \times 10^{31}$	$\sim 1.2 \times 10^{32}$	$\sim 3.7 \times 10^{32}$	$\sim 4.5 \times 10^{32}$	$\sim 1.7 \times 10^{33}$
$\dot{M}_{th}$ (g s^{-1})	$\sim 1.5 \times 10^8$	$\sim 7.5 \times 10^7$	$\sim 1.0 \times 10^8$	$\sim 2.0 \times 10^8$	$\sim 6.35 \times 10^8$	$\sim 7.5 \times 10^8$	$\sim 2.8 \times 10^9$

Table 3. Calculated upper atmosphere parameters at the Roche lobe location and thermal escape and mass-loss rates for the studied 'super-Earths' for heating efficiencies η of 15 per cent (upper part) and 40 per cent (lower part). Because the exobase level of Kepler-11c does not reach r_{L1}, the planet's values at the exobase are given instead.

Parameter	Kepler-11b	Kepler-11c	Kepler-11d	Kepler-11e	Kepler-11f	GJ 1214b	55 Cnc e
r_{L1}/R_{pl}	∼17.95	∼18.05	∼20.24	∼20.96	∼30.24	∼4.26	∼3.82
r_{exo}/R_{pl}		∼14					
T_{L1} (K)	∼670	$T_{exo} \sim 785$	∼353	∼325	∼270	∼1360	∼1415
n_{L1} (cm^{-3})	$\sim 3.7 \times 10^4$	$n_{exo} \sim 7.0 \times 10^3$	$\sim 1.0 \times 10^4$	$\sim 6.5 \times 10^3$	$\sim 9.4 \times 10^4$	$\sim 1.8 \times 10^6$	$\sim 1.0 \times 10^7$
L_{th} (s^{-1})	$\sim 7.0 \times 10^{31}$	$\sim 2.45 \times 10^{31}$	$\sim 6.0 \times 10^{31}$	$\sim 6.5 \times 10^{31}$	$\sim 2.5 \times 10^{32}$	$\sim 4.5 \times 10^{32}$	$\sim 9.8 \times 10^{32}$
$\dot{M}_{th}$ (g s^{-1})	$\sim 1.15 \times 10^8$	$\sim 4.0 \times 10^7$	$\sim 1.0 \times 10^8$	$\sim 1.1 \times 10^8$	$\sim 4.0 \times 10^8$	$\sim 7.5 \times 10^8$	$\sim 1.6 \times 10^9$
r_{exo}/R_{pl}		∼16					
T_{L1} (K)	∼1190	$T_{exo} \sim 1415$	∼650	∼590	∼110	∼2520	∼2890
n_{L1} (cm^{-3})	$\sim 4.8 \times 10^4$	$n_{exo} \sim 9.7 \times 10^3$	$\sim 2.2 \times 10^4$	$\sim 1.2 \times 10^4$	$\sim 7.0 \times 10^4$	$\sim 1.5 \times 10^6$	$\sim 8.8 \times 10^6$
L_{th} (s^{-1})	$\sim 1.26 \times 10^{32}$	$\sim 7.35 \times 10^{31}$	$\sim 1.5 \times 10^{32}$	$\sim 1.5 \times 10^{32}$	$\sim 2.7 \times 10^{32}$	$\sim 9.7 \times 10^{32}$	$\sim 1.4 \times 10^{33}$
$\dot{M}_{th}$ (g s^{-1})	$\sim 2.0 \times 10^8$	$\sim 1.3 \times 10^8$	$\sim 2.5 \times 10^8$	$\sim 2.5 \times 10^8$	$\sim 4.5 \times 10^8$	$\sim 1.5 \times 10^9$	$\sim 2.3 \times 10^9$

40 per cent. For $\eta = 40$ per cent all 'super-Earths' are in the blow-off regime. For the lower heating efficiency of 15 per cent, only Kepler-11c is not in blow-off but experiences strong Jeans-type escape at the exobase level from its non-hydrostatic expanded upper atmosphere which is about a factor of 0.65 lower compared to the hydrodynamic outflow rate at the exobase level. The usual Jeans approach which assumes zero bulk velocity would yield a value which is a factor of 0.145 lower.

Another interesting effect on the exobase temperature can be seen at the most distant 'super-Earth', Kepler-11f where T_{exo} cools adiabatically to a very low value of ∼55 K. However, as mentioned above it is important to note that the results in Table 2 neglect the Roche lobe and its escape-enhancing effects. If we consider this more realistic scenario and compare the exobase levels of the studied 'super-Earths' with the location of the L_1 point r_{L1} shown in Table 3 one can see that all 'super-Earths' except Kepler-11c experience escape due to Roche lobe overflow. This geometrical blow-off is most extreme for 55 Cnc e and is also effective for GJ 1214b for which the distances of the respective L1 points r_{L1} are about $4R_{pl}$. Due to the low gravities, the enormous expansions of the upper atmospheres and the relatively close distances to their host stars, one cannot neglect the Roche lobe effects. Table 3 shows the calculated parameters, but with Roche lobe effects included at the distance of the corresponding L1 points. In such a case the atoms escape as they reach and overflow the Roche lobe.

If we compare the escape rates which neglect the Roche lobe effects shown in Table 2 with those of Table 3 where Roche lobe effects are included, one can see that the stellar tidal forces enhance the atmospheric escape. The escape rates are influenced more strongly at the close-in 'super-Earths' GJ 1214b and 55 Cnc e compared to the Kepler-11 planets where r_{L1} is further away from r_{pl}. One can also see that the temperatures are different at the exobase level for Kepler-11c without (Table 2) and with Roche lobe effects (Table 3). The reason is that with the Roche lobe effects, the radial flow velocity is larger, which results in a larger adiabatic cooling. One should also note that a number density which is less or larger than the assumed 10^{13} cm^{-3} at the homopause level would result in a lower or higher escape rate.

Figs 2 and 3 have the Roche lobe effects included and show the calculated temperature, velocity and density profiles as a function of planetary radii from the homopause distance up to the Roche lobe and in the case of Kepler-11c up to the exobase level. In Fig. 2 we consider a low heating efficiency η of 15 per cent, i.e. the availability of IR-cooling molecules in the upper atmosphere and in Fig. 3 we use a heating efficiency $\eta = 40$ per cent as expected for hydrogen-rich hot gas giants (e.g. Yelle 2004; Koskinen et al. 2012).

One can see in Figs 2(a) and 3(a) that the temperature structure of these 'super-Earth' upper atmospheres is determined by a complex interplay between the XUV flux, the planet's mean density,

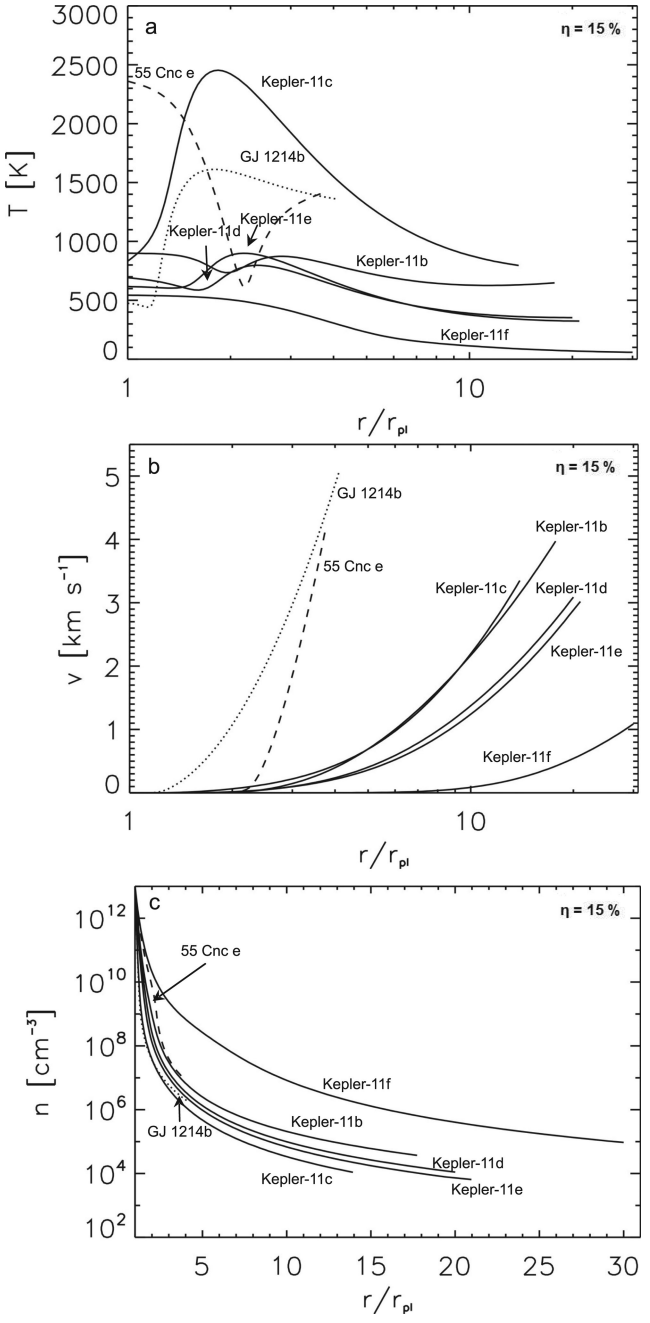

Figure 2. Modeled temperature, velocity and number density profiles of 55 Cnc e, GJ 1214b, Kepler-11b-f from the lower thermosphere up to the Roche lobe distance r_{L1} given in Table 3 for a low heating efficiency with $\eta = 15$ per cent.

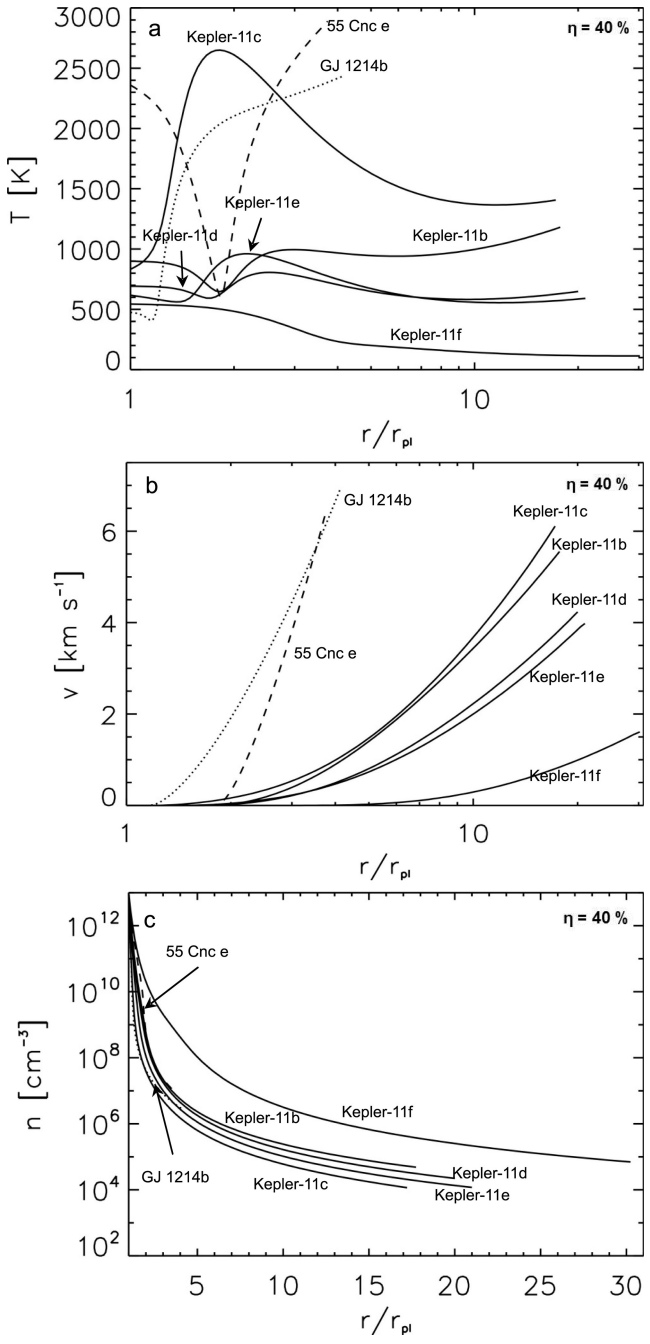

Figure 3. Modelled temperature, velocity and number density profiles of 55 Cnc e, GJ 1214b, Kepler-11b-f from the lower thermosphere up to the Roche lobe distance r_{L1} given in Table 3 for a heating efficiency $\eta = 40$ per cent.

and its skin or equilibrium temperature $T_0 \approx T_{eq}$. In the case of the hottest 'super-Earth' 55 Cnc e the maximum XUV flux is deposited at higher altitudes (see also Fig. 1), therefore, one can see that the temperature first decreases until the XUV radiation heats the atmosphere and expansion related to adiabatic cooling becomes relevant. For Kepler-11c which is the heaviest 'super-Earth' with a cooler skin temperature the XUV flux is deposited at a closer distance so that the atmosphere is heated to a temperature peak which is above 2500 K. Then adiabatic cooling due to hydrodynamic expansion cools the upper atmosphere at large distances to temperatures below 1500 K for an η of 40 per cent and <1000 K if $\eta = 15$ per cent. One can also see that for the 'super-Earth' which is furthest away from its host star, namely Kepler-11f, the temperature decreases until the upper atmosphere reaches the Roche lobe distance. The XUV flux is too low to raise the temperature around the altitude where the maximum energy is deposited. Due to this different behaviour, Kepler-11f is the only 'super-Earth' in our sample where the energy-limited formula in equation (12) underestimates the escape rate. From Figs 2(b) and 3(b) one can see that the expanding hydrogen atoms have velocities of a few km s^{-1} but <10 km s^{-1}. Figs 2(c) and 3(c) show the corresponding number density profiles.

After the investigation of the blow-off regimes and upper atmosphere structures of the seven 'super-Earths' we compare the

Table 4. Estimated hydrogen loss rates from equation (12) for energy-limited escape ($\eta = 100$ per cent) and heating efficiencies of 40 and 15 per cent.

Exoplanet	$\eta = 100$ per cent: $L_{\rm th}$ (s^{-1})	$\eta = 40$ per cent: $L_{\rm th}$ (s^{-1})	$\eta = 15$ per cent: $L_{\rm th}$ (s^{-1})
Kepler-11b	$\sim 6.0 \times 10^{32}$	$\sim 2.4 \times 10^{32}$	$\sim 9.0 \times 10^{31}$
Kepler-11c	$\sim 5.9 \times 10^{32}$	$\sim 2.3 \times 10^{32}$	$\sim 8.9 \times 10^{31}$
Kepler-11d	$\sim 7.5 \times 10^{32}$	$\sim 3.0 \times 10^{32}$	$\sim 1.1 \times 10^{32}$
Kepler-11e	$\sim 8.0 \times 10^{32}$	$\sim 3.2 \times 10^{32}$	$\sim 1.2 \times 10^{32}$
Kepler-11f	$\sim 3.5 \times 10^{32}$	$\sim 1.4 \times 10^{32}$	$\sim 5.3 \times 10^{31}$
GJ 1214b	$\sim 4.6 \times 10^{33}$	$\sim 1.9 \times 10^{33}$	$\sim 7.0 \times 10^{32}$
55 Cnc e	$\sim 1.7 \times 10^{34}$	$\sim 7.0 \times 10^{33}$	$\sim 2.6 \times 10^{33}$

calculated thermal escape rates with escape estimates from the simple energy-limited escape formula (e.g. Watson, Donahue & Walker 1981; Hunten et al. 1987), but introduce a heating efficiency η and a potential energy reduction factor due to the stellar tidal forces (Erkaev et al. 2007)

$$K = 1 - \frac{3}{2(r_{\rm L1}/R_{\rm pl})} + \frac{1}{2(r_{\rm L1}/R_{\rm pl})^3}. \quad (12)$$

The equation can then be written as

$$L_{\rm th} \approx \frac{3\eta I_{\rm XUV} F_{\rm XUV}}{4\, G \rho_{\rm pl} m_{\rm H} K}, \quad (13)$$

where $I_{\rm XUV}$ is the XUV enhancement factor given in Table 1, $F_{\rm XUV}$ is the present time solar XUV flux at 1 au, G is Newton's gravitational constant, $\rho_{\rm pl}$ is the planetary density and $m_{\rm H}$ is the mass of a hydrogen atom. The results are shown in Table 4 for the energy-limited case with $\eta = 100$ per cent and heating efficiencies of 40 and 15 per cent.

The Roche lobe potential energy reduction factor K plays only a role for GJ 1214b and 55 Cnc e because the L_1 point of the Roche lobe is much closer to the planetary surfaces as compared to the other 'super-Earths'. K is 1.53 for GJ 1214b and 1.63 for 55 Cnc e and ~1 for all five Kepler-11 planets. If we compare the thermal escape rates estimated by the simple equation (12) with those obtained by the hydrodynamic model in Table 3, one can see that, besides of Kepler-11f, the atmospheric escape rates are only slightly overestimated. A difference of a factor of 2–3 is certainly within all the other uncertainties such as the XUV flux enhancement. For that reason, our study indicates that the simple formula given in equation (12) is useful for mass-loss estimates of hydrogen-rich exoplanets during evolutionary time-scales, if the particular planet is exposed to a high XUV flux and/or is located at close orbital distance. However, equation (12) should not be used if the atmosphere of a planet is not within the blow-off regime. By comparing the exobase location with the distance of the L_1 point of the most massive 'super-Earth' Kepler-11c, one can see that the exobase does not reach the Roche lobe distance. By considering the Roche lobe effects one can see from Table 3 that the exobase temperature $T_{\rm exo}$ of Kepler-11c is ~785 K for a heating efficiency η of 15 per cent and ~1415 K if η is 40 per cent. The classical critical temperature $T_{\rm c}$ for blow-off can be written as (e.g. Hunten et al. 1987)

$$T_{\rm c} = \frac{2\, G m_{\rm H} M_{\rm pl}}{3 k r_{\rm exo}}. \quad (14)$$

By using the corresponding parameters for Kepler-11c given in Tables 1 and 3, $T_{\rm c}$ is ~1490 K for η=15 per cent and ~1350 K if $\eta = 40$ per cent. The corresponding exobase temperatures $T_{\rm exo}$ for the particular planet are ~785 K and 1415 K, respectively. By using these criteria one finds that the upper atmosphere of Kepler-11c would be in the blow-off stage for the higher heating efficiency but not for the lower value of 15 per cent. However, Erkaev et al. (2007) showed that stellar tidal forces influence also the critical temperature $T_{\rm c}$ so that under certain conditions blow-off can occur. If one follows the derivations related to the potential energy difference between the exobase level and the Roche lobe, given in Erkaev et al. (2007) we obtain the following equation:

$$T_{\rm c}(x) = T_{\rm Jup} \left(\frac{M_{\rm pl} R_{\rm Jup}}{M_{\rm Jup} R_{\rm pl}} \right) \frac{K(x_{L_1}/x)}{x}, \quad (15)$$

with

$$x = \frac{r_{\rm exo}}{R_{\rm pl}} \quad \text{and} \quad x_{L_1} = \frac{r_{L1}}{R_{\rm pl}}. \quad (16)$$

Here $T_{\rm Jup} \sim 1.45 \times 10^5$ K is the critical temperature for the onset of blow-off at the radius of Jupiter (i.e. when $r_{\rm exo} = R_{\rm pl}$), and $M_{\rm Jup}$ and $R_{\rm Jup}$ are the mass and radius of Jupiter. Fig. 4 compares the temperature profiles $T_{\rm c}$ and $T_{\rm c}(x)$ of Kepler-11c as a function of planetary radius without and with Roche lobe effects. From this one can see that Roche lobe effects reduce the critical temperature $T_{\rm c}(x)$ at the exobase level to ~80 K for a heating efficiency η of 15 per cent, resulting in an environment where Kepler-11c's upper atmosphere will experience blow-off. But it is interesting to note that equation (12) overestimates in that particular case the atmospheric escape rate by a factor of ~3.6.

Compared to the mass-loss estimations of 'hot Jupiters' such as HD 209458b which are of the order of ~2–5 $\times$ 10^{10} g s^{-1} (e.g.

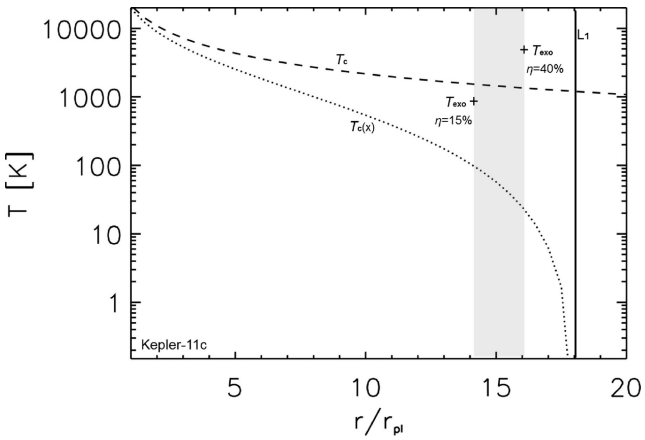

Figure 4. Comparison of the critical temperature $T_{\rm c}$ without (dashed line) and $T_{\rm c}(x)$ with Roche lobe effects (dotted line) at Kepler-11c as a function of planetary radii. The symbol '+' corresponds to $T_{\rm exo}$ related to the low and higher η values. The vertical solid line corresponds to the Roche lobe distance for the L_1 point and the shaded area marks the exobase levels of Kepler-11c for heating efficiencies η of 15 per cent and 40 per cent, respectively.

Yelle 2004; Tian et al. 2005a; García Muñoz 2007; Penz et al. 2008; Lammer et al. 2009a; Koskinen et al. 2012) the mass-loss of the studied 'super-Earths' is ∼10–100 times lower. The main reasons are that the studied 'super-Earths' are exposed to lower XUV fluxes and the mean density of HD 209458b is lower.

4 CONCLUSION

We studied the blow-off regimes of seven hydrogen-rich 'super-Earths' with known sizes and masses by applying a 1D hydrodynamic upper atmosphere model which includes tidal forces. The upper atmosphere temperature profiles of these hydrogen-rich 'super-Earths' are determined by a complex interplay between the equilibrium or skin temperature of the particular planet, the homopause number density, the stellar XUV flux, the height where the maximum XUV energy is deposited, adiabatic cooling, the mean density of the particular planet, and the Roche lobe distance. The upper atmospheres of Kepler-11b, Kepler-11d, Kepler-11e, Kepler-11f, GJ 1214b and 55 Cnc e expand up to the L_1 points of their Roche lobes, which enhances their atmospheric escape rates. Kepler-11c is the only 'super-Earth' in our sample where its exobase level does not reach the Roche lobe. The thermal mass-loss rates of GJ 1214b and 55 Cnc e are ∼10 times lower and about 100 times lower for the Kepler-11 'super-Earths', respectively, compared to a typical 'hot Jupiter' such as HD 209458b. By comparing the escape rates obtained by the hydrodynamic upper atmosphere model with the modified energy-limited equation given in Erkaev et al. (2007) and Lammer et al. (2009) we found that besides of Kepler-11c and Kepler-11f and 55 Cnc e the escape rates are overestimated by about a factor of 2, which lies within all other parametrical uncertainties. However, our study also indicates that the energy-limited equation should only be applied for hydrogen-rich exoplanets which have a hot skin or equilibrium temperature and/or are exposed to high XUV flux values. From our results one can expect that the mass of the investigated 'super-Earths' will not be affected strongly by atmospheric mass-loss during their remaining lifetimes.

ACKNOWLEDGMENTS

NVE, KGK, MLK and HL acknowledge the support by the FWF NFN project S116 'Pathways to Habitability: From Disks to Active Stars, Planets and Life', and the related FWF NFN subprojects, S116 606-N16 'Magnetospheric Electrodynamics of Exoplanets' and S116607-N16 'Particle/Radiative Interactions with Upper Atmospheres of Planetary Bodies Under Extreme Stellar Conditions'. KGK, HL and PO thank also the Helmholtz Alliance project 'Planetary Evolution and Life'. ML and PO acknowledge support from the FWF project P22950-N16. NVE acknowledges support by the RFBR grant No 12-05-00152-a. The authors also acknowledge support from the EU FP7 project IMPEx (No.262863) and the EUROPLANET-RI projects, JRA3/EMDAF and the Na2 science working group WG5. The authors thank the International Space Science Institute (ISSI) in Bern, and the ISSI team 'Characterizing stellar- and exoplanetary environments'. Finally, we thank an anonymous referee for interesting suggestions and recommendations which helped to improve the article.

REFERENCES

Atreya S. K., 1986, Atmospheres and Ionospheres of the Outer Planets and their Satellites. Springer Publishing House, Heidelberg, Berlin, New York
Atreya S. K., 1999, Eos Trans. Am. Geophys. Union, 80, 320
Baraffe I., Selsis F., Chabrier G., Barman T. S., Allard F., Hauschildt P. H., Lammer H., 2004, A&A, 419, L13
Batalha N. M. et al., 2011, ApJ, 729, 27
Bauer S. J., 1971, Nat, 232, 101
Bauer S. J., Lammer H., 2004, Planetary Aronomy: Atmosphere Environments in Planetary Systems. Springer Publishing House, Berlin, Heidelberg, New York
Bean J. L., Miller-Ricci K. E., Homeier D., 2010, Nat, 468, 669
Bean J. L. et al., 2011, ApJ, 743, 92
Ben-Jaffel L., 2007, ApJ, 671, L61
Ben-Jaffel L., Sona Hosseini S., 2010, ApJ, 709, 1284
Cecchi-Pestellini C., Ciaravella A., Micela G., Penz T., 2009, A&A, 496, 863
Chamberlain J. W., 1963, Planet. Space. Sci., 11, 901
Charbonneau D. et al., 2009, Nat, 462, 891
Chassefière E., 1996a, J. Geophys. Res., 101, 26039
Chassefière E., 1996b, Icarus, 124, 537
Cochran W. D. et al., 2011, ApJ, 197, 7
Croll B., Albert L., Jayawardhana R., Miller-Ricci K., Fortney J. J., Murray N., Neilson H., 2011, ApJ, 736, 78
Davis T. A., Wheatley P. J., 2009, MNRAS, 396, 1012
de Mooij E. J. W. et al., 2012, A&A, 538, A46
Demory B.-O., Gillon M., Seager S., Benneke B., Deming D., Jackson B., 2012, ApJ, 751, L28
Désert J.-M. et al., 2011, ApJ, 731, L40
Ekenbäck A., Holmström M., Wurz P., Grießmeier J.-M., Lammer H., Selsis F., Penz T., 2010, ApJ, 709, 670
Endl M. et al., 2012, ApJ, 759, 19
Engle S. G., Guinan E. F., 2011, in Qain S., Leung K., Zhu L., Kwok S., eds, 9th Pacific Rim Conference on Stellar Astrophysics, ASP Conf. Ser. Vol. 451, Astron. Soc. Pac., San Francisco, p. 285
Erkaev N. V., Kulikov Yu. N., Lammer H., Selsis F., Langmayr D., Jaritz G. F., Biernat H. K., 2007, A&A, 472, 329
Fossati L. et al., 2010, ApJ, 714, L222
Fressin F. et al., 2012, Nat, 482, 195
García Muñoz A., 2007, Planet. Space Sci., 55, 1426
Gillon M. et al., 2012, A&A, 539, A28
Gross S. H., 1972, J. Atmos. Sci., 29, 214
Holmström M., Ekenbäck A., Selsis F., Penz T., Lammer H., Wurz P., 2008, Nat, 451, 670
Hubbard W. B., Hattori M. F., Burrows A., Hubeny I., 2007, ApJ, 658, L59
Hunten D. M., Pepin R. O., Walker J. C. G., 1987, Icarus, 69, 532
Ikoma M., Hori Y., 2012, ApJ, 753, 66
Jackson B., Miller N., Barnes R., Raymond S. N., Fortney J., Greenberg R., 2010, MNRAS, 407, 910
Kasting J. F., Pollack J. B., 1983, Icarus, 53, 479
Khodachenko M. L. et al., 2007, Planet. Space Sci., 55, 631
Koskinen T. T., Aylward A. D., Miller S., 2007, Nat, 450, 845
Koskinen T. T., Yelle R. V., Lavvas P., Lewis N. K., 2010, ApJ, 723, 116
Koskinen T. T., Harris M. J., Yelle R. V., Lavvas P., 2012, Icarus, accepted (arXiv:1210.1536)
Kuchner M. J., 2003, ApJ, 596, L105
Lammer H., 2012, Origin and Evolution of Planetary Atmospheres: Implications for Habitability, Springer Briefs in Astronomy, Springer Pub. House, Berlin, Heidelberg, New York
Lammer H., Selsis F., Ribas I., Guinan E. F., Bauer S. J., Weiss W. W., 2003, ApJ, 598, L121
Lammer H., Kasting J. F., Chassefière E., Johnson R. E., Kulikov Yu. N., Tian F., 2008, Space Sci. Rev., 139, 399
Lammer H. et al., 2009a, A&A, 506, 399
Lammer H. et al., 2009b, A&AR, 17, 181
Lammer H., Kislyakova K. G., Holmström H., Khodachenko M. L., Grießmeier J.-M., 2011, Astrophys. Space Sci., 335, 9
Lammer H. et al., 2012, Orig. Life Evol. Biosph., 41, 503
Lecavelier Des Etangs A., 2007, A&A, 461, 1185
Lecavelier des Etangs A., Vidal-Madjar A., McConnell J. C., Hébrard G., 2004, A&A, 418, L1

Lecavelier des Etangs A. et al., 2010, A&A, 514, A72
Léger A. et al., 2009, A&A, 506, 287
Leitzinger M. et al., 2011, Planet. Space Sci., 59, 1472
Linsky J. L., Yang H., France K., Froning C. S., Green J. C., Stocke J. T., Osterman S. N., 2010, ApJ, 717, 1291
Lissauer J. J. et al., 2011, Nat, 470, 53
Madhusudhan N., Lee K. K. M., Mousis O., 2012, ApJ, 759, L40
Miller-Ricci E., Fortney J. J., 2010, ApJ, 716, L74
Murray-Clay R. A., Chiang E. I., Murray N., 2009, ApJ, 693, 23
Nettelmann N., Kramm U., Redmer R., Neuhäuser R., 2010, A&A, 523, A26
Nettelmann N., Fortney J. J., Kramm U., Redmer R., 2011, ApJ, 733, 2
Öpik E. J., 1963, Geophys. J. Roy. Astron. Soc., 7, 490
Owen J. E., Jackson A. P., 2012, MNRAS, 425, 2931
Penz T., Micela G., 2008, A&A, 479, 579
Penz T. et al., 2008a, Planet. Space Sci, 56, 1260
Penz T., Micela G., Lammer H., 2008b, A&A, 477, 309
Pepin R. O., 1991, Icarus, 92, 2
Pepin R. O., 2000, Space Sci. Rev., 92, 371
Pierrehumbert R., Gaidos E., 2011, ApJ, 734, L13
Ribas I., Guinan E. F., Güdel M., Audard M., 2005, ApJ, 622, 680
Sanz-Forcada J., Micela G., Ribas I., Pollock A. M. T., Eiroa C., Velasco A., Solano E., Garcia-Alvarez D., 2011, A&A, 532, A6
Sekiya M., Nakazawa K., Hayashi C., 1980, Prog. Theor. Phys., 64, 1968
Sekiya M., Hayashi C., Nakazawa K., 1981, Prog. Theor. Phys., 66, 1301
Tian F., Toon O. B., Pavlov A. A., De Sterck H., 2005a, ApJ, 621, 1049
Tian F., Toon O. B., Pavlov A. A., De Sterck H., 2005b, Sci, 308, 1014
Tian F., Kasting J. F., Liu H., Roble R. G., 2008a, J. Geophys. Res., 113, E05008
Tian F., Solomon S. C., Qian L., Lei J., Roble R. G., 2008b, J. Geophys. Res., 113, E07005
Valencia D., Ikoma M., Guillot T., Nettlemann N., 2010, A&A, 516, A20
Vidal-Madjar A., Lecavelier des Etangs A., Désert J. M., Ballester G. E., Ferlet R., Hébrard G., Mayor M., 2003, Nat, 422, 143
Vidal-Madjar A. et al., 2004, ApJ, 604, L69
Volkov A. N., Tucker O. J., Erwin J. T., Johnson R. E., 2011, Phys. Fluids, 23, 066601
von Braun K. et al., 2011, ApJ, 740, 49
Watson A. J., Donahue T. M., Walker J. C. G., 1981, Icarus, 48, 150
Wordsworth R., 2012, Icarus 219, 267
Yamanaka M. D., 1995, Adv. Space Res., 15, 47
Yelle R. V., 2004, Icarus, 170, 167

This paper has been typeset from a TEX/LATEX file prepared by the author.